

Protection of Weyl Semimetals in Optical Lattices by Gauge-Color-Translation Symmetry

Jing-Min Hou*

Department of Physics, Southeast University, Nanjing, 211189, China

(Dated: December 19, 2012)

We study three tight-binding models of two-dimensional fermionic optical lattices. We find that these systems have a novel composite symmetry, i.e. gauge-color-translation (GCT) symmetry, which consists of a fixed translation transformation, a color transformation and a fixed local $U(1)$ gauge transformation. The corresponding symmetry operator is antiunitary. We predict that, due to the protection of GCT symmetry, the conduction and valence bands are degenerate at some isolated momenta. These degenerate points form Weyl nodes in the Brillouin zone. The quasiparticles and quasiholes near the Weyl nodes can be considered as Weyl fermions and have chirality characterized by a winding number. With the protection of GCT symmetry and the winding number, the Weyl nodes occur in a very large range of parameters.

PACS numbers: 02.20.-a, 03.65.Vf, 03.75.Ss, 05.30.Fk

Introduction.—The research on topological phases is becoming an increasingly important theme in condensed matters. Topological matters are classified according to topological invariants rather than symmetries[1, 2]. More recently, physicists have found that, besides the gapped systems, gapless systems can also support topological phases, i.e., topological semimetals[3–12]. Semimetals are characterized by the presence of point nodes in the band structures, that is, two distinct bands touch each other at some isolated points in momentum space.

Weyl semimetal is a class of topological semimetals. For Weyl semimetals, near the band-degeneracy points (also called Weyl nodes), the single particle Hamiltonian can be written as $h(\mathbf{k}) = \sum_{ij} v_{ij} k_i \sigma_j$, with \mathbf{k} and $\boldsymbol{\sigma}$ being the wave vector and the Pauli matrix, respectively. That is to say, near these touching points the dispersion relation is linear and can be described by a massless two-component Weyl Hamiltonian. Near the Weyl nodes, the quasiparticles are Weyl fermions and have chirality characterized by a winding number defined as

$$w = \text{sgn}[\det(v_{ij})] = \pm 1. \quad (1)$$

Due to the theorem of Nielsen and Ninomiya, Weyl nodes always occur in pairs of opposite chirality[13]. In Weyl semimetals, Weyl nodes with opposite chirality are separated from each other in momentum space and thus can not be destroyed by mutual annihilation of pairs with opposite topological charges.

In three dimensions, the band degeneracy at Weyl nodes can be accidental [14] or protected by symmetries. The robustness of the accidental degeneracy depends on its co-dimension[5]. To achieve a two-band accidental degeneracy, three real parameters are required to be tuned. Thus, such accidental band degeneracies are vanishingly improbable in one and two dimensions if there are not additional symmetry constraints[15]. Therefore, in two dimensions, the band degeneracy at Weyl nodes must be protected by symmetries. In general, the band degeneracies are protected by point groups or time reversal symmetry.

In this Letter, we will show that, besides point groups and time-reversal symmetry, there is another kind of symmetry, gauge-color-translation (GCT) symmetry, to protect band degeneracies in condensed matters. GCT symmetry protected Weyl nodes are ubiquitous in condensed matters, but which are rarely studied by physicists before. GCT symmetry is a composite symmetry; its symmetry operator is a combined operation and consists of a translation transformation, a color transformation and a local gauge transformation in sequence. Sometimes, the local gauge transformation is not necessary, which can be regarded as a trivial case with a global gauge transformation. GCT operator has the form as $\Gamma = GCT_{\boldsymbol{\tau}}$, where $T_{\boldsymbol{\tau}}$ is a translation operator such as $T_{\boldsymbol{\tau}}\mathbf{r} = \mathbf{r} + \boldsymbol{\tau}$, C is a color transformation like $\sigma_x K$ with K and σ_x being the complex conjugation and pauli matrix, respectively, and G is a fixed local gauge transformation. Here, we stress that GCT symmetry is an antiunitary symmetry, i.e., its symmetry operator is antiunitary, because it includes the complex conjugation K . GCT symmetry operator Γ and the space group of the lattice can make up a generalized color space group, where a color transformation is always followed by a local gauge transformation. However, only GCT symmetry is responsible for protecting Weyl nodes. Thus, here we mainly consider GCT symmetry.

In order to present GCT symmetry protected Weyl nodes, we first consider a two-dimensional rectangular optical lattice as shown in Fig.1(a), denoted as Model 1. We will show that Weyl semimetals appear in this model. In order to show ubiquity of GCT symmetry protected Weyl nodes in condensed matters, we will also briefly investigate and discuss two other two-dimensional rectangular lattices, denoted as Models 2 and 3, respectively, as shown in Fig.1(b) and (c), which also support the existence of Weyl semimetals. These models can experimentally be realized and detected in optical lattices with

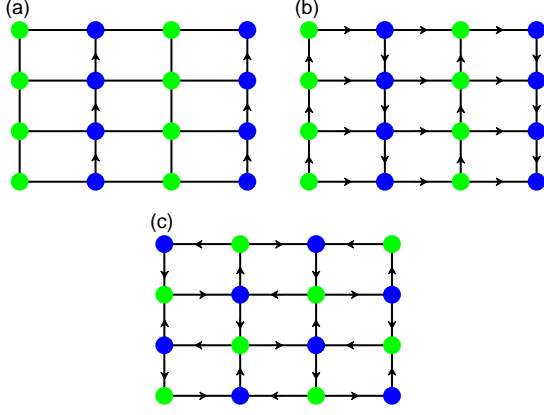


FIG. 1: (Color online). Schematic of the rectangular optical lattices and the designed phase factor (denoted by arrows) for (a) Model 1, (b) Model 2, and (c) Model 3. Here, the green and blue balls represent the lattice sites of sublattices A and B , respectively.

laser-assisted tunneling as proposed in Reference [16].

Model.—Model 1 consists of two sublattices denoted as A and B , respectively. The two sublattices have the lattice spacings $2d_x$ and d_y in the x and y directions, respectively. For sublattice B , along y direction, there exists a phase factor between two neighbor lattice sites. For each sublattice, the primitive lattice vectors are defined as $\mathbf{a}_1 = (2d_x, 0)$ and $\mathbf{a}_2 = (0, d_y)$. The lattice vectors can be expressed as $\mathbf{R}_n = n_1\mathbf{a}_1 + n_2\mathbf{a}_2$ with n_1 and n_2 being integers. we chose a lattice site in sublattice A as the origin, then the lattice vectors in sublattice A and sublattice B can be rewritten as $\mathbf{R}_n^A = \mathbf{R}_n$ and $\mathbf{R}_n^B = \mathbf{R}_n + \mathbf{a}_1/2$.

The tight-binding Hamiltonian for Model 1 can be written as,

$$H = - \sum_{i \in A} [J_{i, i+\hat{x}} a_i^\dagger a_{i+\hat{x}} + J_{i, i+\hat{y}} a_i^\dagger a_{i+\hat{y}} + J_{i+\hat{x}, i+\hat{x}+\hat{y}} b_{i+\hat{x}}^\dagger b_{i+\hat{x}+\hat{y}} + J_{i, i+\hat{x}} a_i^\dagger b_{i+\hat{x}} + J_{i+\hat{x}, i+2\hat{x}} b_{i+\hat{x}}^\dagger a_{i+2\hat{x}} + \text{H.c.}], \quad (2)$$

with $J_{i, i+\hat{x}} = t_x$, $J_{i, i+\hat{y}} = t_y$ for $i \in A$ and $t_y e^{-i\gamma}$ for $i \in B$. Here, a_i is the annihilation operator that destructs a particle with the Wannier state $w_i^A(\mathbf{r}) = w_0^A(\mathbf{r} - \mathbf{R}_i^A)$ located at the site i in sublattice A and b_j the annihilation operator destructing a particle with the Wannier state $w_j^B(\mathbf{r}) = w_0^B(\mathbf{r} - \mathbf{R}_j^B)$ located at the site j in sublattice B ; the subscript $i \equiv (i_x, i_y)$ is the coordinate for the sites of sublattice A with the primitive lattice vectors \mathbf{a}_1 and \mathbf{a}_2 as the bases; $\hat{x} = (1/2, 0)$ and $\hat{y} = (0, 1)$ represent the vectors between the neighbor lattice sites in the whole lattice; $0 < \gamma < 2\pi$ is a phase factor along with tunneling; t_x and t_y are the hopping amplitudes along the x and y directions, respectively.

This system is invariant under a GCT transformation, i.e. $H = \Gamma H \Gamma^{-1}$, where the symmetry operator Γ is

defined as follows,

$$\Gamma = (e^{i\gamma})^{i_y} \sigma_x K T_{\mathbf{a}_1/2}, \quad (3)$$

where $(e^{i\gamma})^{i_y}$ is a local $U(1)$ gauge transformation. The corresponding inverse operator is $\Gamma^{-1} = (e^{i\gamma})^{i_y} \sigma_x K T_{\mathbf{a}_1/2}^{-1}$. The GCT operator has the character as follows,

$$\Gamma^2 = T_{\mathbf{a}_1}, \quad (4)$$

where $T_{\mathbf{a}_1} = \{E|\mathbf{a}_1\}$.

Band structure and Bloch functions.—In the reciprocal lattice, the reciprocal lattice vectors are defined as $\mathbf{K}_m = m_1\mathbf{b}_1 + m_2\mathbf{b}_2$, where m_1 and m_2 are integers, and $\mathbf{b}_1 = (\pi/d_x, 0)$ and $\mathbf{b}_2 = (0, 2\pi/d_y)$ are the corresponding primitive reciprocal lattice vectors. Thus, the Brillouin zone is $-\pi/2d_x \leq k_x \leq \pi/2d_x$, $-\pi/d_y \leq k_y \leq \pi/d_y$. The corresponding Bloch functions for the A and B sublattices can be written as $\psi_{\mathbf{k}}^A(\mathbf{r}) = \frac{1}{\sqrt{N}} \sum_i e^{i\mathbf{k} \cdot \mathbf{r}} w_i^A(\mathbf{r} - \mathbf{R}_i^A)$ and $\psi_{\mathbf{k}}^B(\mathbf{r}) = \frac{1}{\sqrt{N}} \sum_i e^{i\mathbf{k} \cdot (\mathbf{r} + \mathbf{a}_1/2)} w_i^B(\mathbf{r} + \mathbf{a}_1/2 - \mathbf{R}_i^B)$, respectively, where N is the number of lattice sites in each sublattice. Correspondingly, we have the annihilation operators as $a_{\mathbf{k}} = \frac{1}{\sqrt{N}} \sum_i a_i e^{-i\mathbf{k} \cdot \mathbf{R}_i^A}$ and $b_{\mathbf{k}} = \frac{1}{\sqrt{N}} \sum_i b_i e^{-i\mathbf{k} \cdot \mathbf{R}_i^B}$, which destruct a particle in the Bloch states $\psi_{\mathbf{k}}^A(\mathbf{r})$ and $\psi_{\mathbf{k}}^B(\mathbf{r})$, respectively. We define the two-component annihilation operator as $\eta_{\mathbf{k}} \equiv \frac{1}{\sqrt{2}}[a_{\mathbf{k}} + ib_{\mathbf{k}}, ia_{\mathbf{k}} + b_{\mathbf{k}}]^T$. The Hamiltonian (2) can be rewritten as $H = \sum_{\mathbf{k}} \eta_{\mathbf{k}}^\dagger \mathcal{H}(\mathbf{k}) \eta_{\mathbf{k}}$ with

$$\mathcal{H}(\mathbf{k}) = -t_y [\cos(k_y d_y) + \cos(k_y d_y - \gamma)] I - 2t_x \cos(k_x d_x) \sigma_x - t_y [\cos(k_y d_y) - \cos(k_y d_y - \gamma)] \sigma_y, \quad (5)$$

and σ_x and σ_y are the Pauli matrices and I the unit matrix.

Diagonalizing Eq.(5), we obtain the dispersion relation as $E(\mathbf{k}) = -t_y [\cos(k_y d_y) + \cos(k_y d_y - \gamma)] \pm t_y \sqrt{4f^2 \cos^2(k_x d_x) + [\cos(k_y d_y) - \cos(k_y d_y - \gamma)]^2}$ with $f = t_x/t_y$. Fig.2 shows this dispersion relation for the cases with $\gamma = \pi$ and $\gamma = 3\pi/5$. We assume that $[c_{\mathbf{k}}^{(1)}, c_{\mathbf{k}}^{(2)}]^T$ is the eigenvector of the Hamiltonian (5) corresponding to eigenenergy $E(\mathbf{k})$, then the Bloch function of the whole lattice can be expressed as

$$\Psi_{\mathbf{k}}(\mathbf{r}) \equiv \begin{pmatrix} u_1(\mathbf{r}) \\ u_2(\mathbf{r}) \end{pmatrix} e^{i\mathbf{k} \cdot \mathbf{r}} = \begin{pmatrix} c_{\mathbf{k}}^{(1)} \psi_{\mathbf{k}}^A(\mathbf{r}) - c_{\mathbf{k}}^{(2)} i \psi_{\mathbf{k}}^A(\mathbf{r}) \\ -c_{\mathbf{k}}^{(1)} i \psi_{\mathbf{k}}^B(\mathbf{r}) + c_{\mathbf{k}}^{(2)} \psi_{\mathbf{k}}^B(\mathbf{r}) \end{pmatrix}, \quad (6)$$

where $u_i(\mathbf{r}) = u_i(\mathbf{r} + \mathbf{R}_n)$. In the momentum space, the Bloch state $\Psi_{\mathbf{k}}(\mathbf{r})$ and eigenenergy $E(\mathbf{k})$ are periodic for reciprocal lattice vectors, i.e. $\Psi_{\mathbf{k}}(\mathbf{r}) = \Psi_{\mathbf{k} + \mathbf{K}_m}(\mathbf{r})$ and $E(\mathbf{k}) = E(\mathbf{k} + \mathbf{K}_m)$.

Weyl semimetals.—From the dispersion relation, we find that the conduction and valence bands are touched at $\mathbf{W}_1 = (-\pi/2d_x, \gamma/2d_y)$, $\mathbf{W}_2 = (\pi/2d_x, \gamma/2d_y)$, $\mathbf{W}_3 = (-\pi/2d_x, \gamma/2d_y - \pi/d_y)$ and $\mathbf{W}_4 = (\pi/2d_x, \gamma/2d_y - \pi/d_y)$

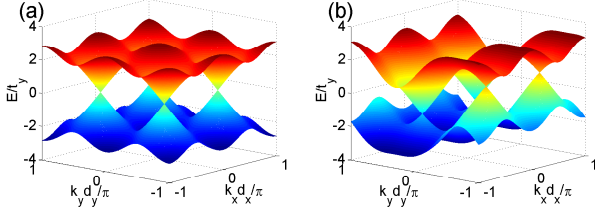


FIG. 2: (Color online). The energy dispersions of Model 1 for (a) $\gamma = \pi$ and (b) $\gamma = 3\pi/5$. Here, $t_x = t_y$ is assumed.

in the Brillouin zone. Near these degenerate points, the single-particle Hamiltonian (5) can be linearized as

$$h(\mathbf{p}) = \pm 2t_y \cos(\gamma/2)I \pm 2t_y f d_x p_x \sigma_x \pm 2t_y \sin(\gamma/2) d_y p_y \sigma_y, \quad (7)$$

where the signs before the three terms make up four combinations such as $(-, -, +)$, $(-, +, +)$, $(+, -, -)$, and $(+, +, -)$ representing the linearized Hamiltonian near the touched points \mathbf{W}_1 , \mathbf{W}_2 , \mathbf{W}_3 , and \mathbf{W}_4 , respectively. The Hamiltonian (7) has the form of Weyl's Hamiltonian and the four Weyl nodes which are located at the boundary of the Brillouin zone. Because the relations $\mathbf{W}_2 = \mathbf{W}_1 + \mathbf{b}_1$ and $\mathbf{W}_4 = \mathbf{W}_3 + \mathbf{b}_1$, \mathbf{W}_1 is equivalent with \mathbf{W}_2 , and \mathbf{W}_3 equivalent with \mathbf{W}_4 , i.e., there are only two unequivalent Weyl nodes in the Brillouin zone. From the definition of the chirality as Eq.(1), we have $w = -1, +1, -1, +1$ for Weyl nodes \mathbf{W}_1 , \mathbf{W}_2 , \mathbf{W}_3 , and \mathbf{W}_4 , respectively. We find that \mathbf{W}_1 and \mathbf{W}_2 , \mathbf{W}_3 and \mathbf{W}_4 are equivalent points but have opposite chirality. Thus, we conclude that the chirality is not absolute in our model, which can be changed through a gauge transformation. However, due to the theorem of Nielsen and Ninomiya[13], in any gauge, the two unequivalent Weyl nodes have opposite chirality.

The Weyl nodes can also interpreted as topological defects of the planar vector field in momentum space like $\mathbf{h} = (-2t_y f \cos(k_x d_x), -t_y [\cos(k_y d_y) - \cos(k_y d_y - \gamma)])$, which is defined by using the coefficients of the Pauli matrices in Eq.(5). The corresponding topological invariant is the winding number defined as $w = \oint_C \frac{d\mathbf{k}}{2\pi} \cdot \mathbf{F}(\mathbf{k})$ with $\mathbf{F}(\mathbf{k}) = \frac{h_x}{|\mathbf{h}|} \nabla \left(\frac{h_y}{|\mathbf{h}|} \right) - \frac{h_y}{|\mathbf{h}|} \nabla \left(\frac{h_x}{|\mathbf{h}|} \right)$ [9]. These vortices have the values of winding number ± 1 , which is consistent with the chirality defined in Eq.(1). Fig.3 shows the vector fields $\mathbf{F}(\mathbf{k})$ for the cases with $\gamma = \pi$ and $\gamma = 3\pi/5$, which manifest the vortex structures indicating the appearing of Weyl nodes.

Symmetry protection.—The Weyl nodes in our systems manifest strong robustness. Firstly, the Weyl nodes appear and the band structure keep gapless for all ranges of $0 < \gamma < 2\pi$. Secondly, any values of the lattice constants d_x and d_y can support Weyl nodes. Besides the protection of topological invariant, these Weyl nodes are protected by GCT symmetry, the operator Γ of which is

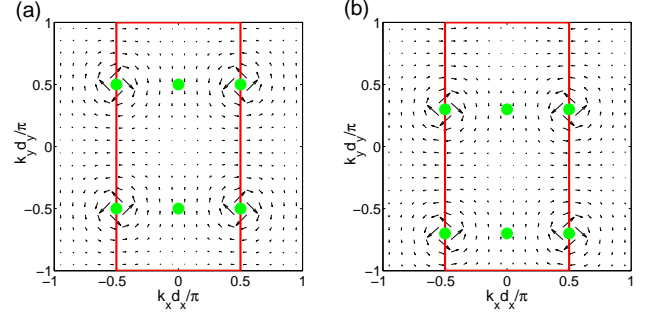


FIG. 3: (Color online). The vortex structures of the vector fields $\mathbf{F}(\mathbf{k})$ for Model 1 with (a) $\gamma = \pi$ and (b) $\gamma = 3\pi/5$. Here, the region surrounded by red lines is the first Brillouin zone; the green balls mark the GCT-invariant points in the first Brillouin zone; the vortices indicate the appearing of Weyl nodes.

expressed in Eq.(3).

The GCT operator Γ acts on the Bloch function (6) as follows

$$\begin{aligned} \Gamma \Psi_{\mathbf{k}}(\mathbf{r}) &= \begin{pmatrix} u_{\mathbf{k}}^{(2)*}(\mathbf{r} - \mathbf{a}_1/2) e^{ik_x d_x} \\ u_{\mathbf{k}}^{(1)*}(\mathbf{r} - \mathbf{a}_1/2) e^{ik_x d_x} \end{pmatrix} e^{-i[k_x x + (k_y - \gamma/d_y)y]} \\ &= \Psi'_{\mathbf{k}'}(\mathbf{r}), \end{aligned} \quad (8)$$

where $x = i_x d_x$ and $y = i_y d_y$. Because Γ is the symmetry operator of the system, $\Psi'_{\mathbf{k}'}(\mathbf{r})$ must be a Bloch wave function of the system. Thus we obtain $u_{\mathbf{k}'}^{(1)}(\mathbf{r}) = u_{\mathbf{k}}^{(2)*}(\mathbf{r} - \mathbf{a}_1/2) e^{ik_x d_x}$ and $u_{\mathbf{k}'}^{(2)}(\mathbf{r}) = u_{\mathbf{k}}^{(1)*}(\mathbf{r} - \mathbf{a}_1/2) e^{ik_x d_x}$, $k'_x = -k_x$ and $k'_y = \gamma/d_y - k_y$.

From Eqs. (6) and (8), it is easy to show that the operator Γ has the effect when acting on the wave vector $\mathbf{k} = (k_x, k_y)$ as $\Gamma : (k_x, k_y) \rightarrow (-k_x, \gamma/d_y - k_y)$. If $\mathbf{k}' = \mathbf{k} + \mathbf{K}_m$, then we can say that \mathbf{k} is an invariant point under GCT transformation. In the Brillouin zone, the GCT-invariant wave vectors are $\mathbf{G}_{1,2} = (\pm\pi/2d_x, \gamma/2d_y)$, $\mathbf{G}_{3,4} = (\pm\pi/2d_x, (\gamma/2 - \pi)/d_y)$, $\mathbf{G}_5 = (0, \gamma/2d_y)$, $\mathbf{G}_6 = (0, (\gamma/2 - \pi)/d_y)$, which are marked by green balls in Fig.3. For the case $\mathbf{k}' = \mathbf{k} + \mathbf{K}_m$, i.e. at the GCT-invariant point \mathbf{G}_i , we have $\Gamma \Psi_{\mathbf{G}_i}(\mathbf{r}) = \Psi'_{\mathbf{G}_i}(\mathbf{r})$. Thus, $\Psi_{\mathbf{G}_i}(\mathbf{r})$ and $\Psi'_{\mathbf{G}_i}(\mathbf{r})$ are both the eigenstates of Hamiltonian H and have the same eigenenergy $E(\mathbf{G}_i)$. Considering Eq.(4), we have $\Gamma^2 \Psi_{\mathbf{G}_i}(\mathbf{r}) = T_{\mathbf{a}_1} \Psi_{\mathbf{G}_i}(\mathbf{r}) = e^{-2iG_{ix} d_x} \Psi_{\mathbf{G}_i}(\mathbf{r})$, where G_{ix} is the x component of \mathbf{G}_i . We define (ψ, φ) as the inner product of the two wave functions ψ and φ . The antiunitary operator Γ has the property that $(\Gamma\psi, \Gamma\varphi) = (\psi, \varphi)^* = (\varphi, \psi)$. Therefore, we have

$$\begin{aligned} (\Psi'_{\mathbf{G}_i}, \Psi_{\mathbf{G}_i}) &= (\Gamma \Psi_{\mathbf{G}_i}, \Gamma \Psi'_{\mathbf{G}_i}) = (\Gamma \Psi_{\mathbf{G}_i}, \Gamma^2 \Psi_{\mathbf{G}_i}) \\ &= e^{-2iG_{ix} d_x} (\Psi'_{\mathbf{G}_i}, \Psi_{\mathbf{G}_i}). \end{aligned} \quad (9)$$

For the case with $G_{ix} = 0$, such as \mathbf{G}_5 and \mathbf{G}_6 , $(\Psi'_{\mathbf{G}_i}, \Psi_{\mathbf{G}_i})$ is unconstrained. For the case with $G_{ix} \neq 0$, such as $\mathbf{G}_1, \mathbf{G}_2, \mathbf{G}_3$ and \mathbf{G}_4 , we obtain the solution

$(\Psi'_{\mathbf{G}_i}, \Psi_{\mathbf{G}_i}) = 0$, that is to say, $\Psi'_{\mathbf{G}_i}$ and $\Psi_{\mathbf{G}_i}$ are orthogonal to each other. Therefore, we arrive at the conclusion that the system must be degenerate at points $\mathbf{G}_{1,2} = (\pm\pi/2d_x, \gamma/2d_y)$ and $\mathbf{G}_{3,4} = (\pm\pi/2d_x, (\gamma/2 - \pi)/d_y)$ in the Brillouin zone, which are just the Weyl nodes $\mathbf{W}_1, \mathbf{W}_2, \mathbf{W}_3$, and \mathbf{W}_4 .

Other models — Besides the above model, there are other models, such as Models 2 and 3 shown in Fig.1, that have similar composite symmetry and the corresponding symmetry protected Weyl nodes. Model 2 has the same sublattices and the same Brillouin zone with Model 1. Thus, its tight-binding Hamiltonian is similar with Eq.(2) but with $J_{i,i+\hat{x}} = t_x e^{-i\beta}$, $J_{i,i+\hat{y}} = t_y e^{-i\gamma}$ for $i \in A$ and $t_y e^{i\gamma}$ for $i \in B$, where $0 < \beta, \gamma < \pi$. This model has the spectrum as $E'(\mathbf{k}) = -t_y[\cos(k_y d_y - \gamma) + \cos(k_y d_y + \gamma)] \pm t_y \sqrt{4f^2 \cos^2(k_x d_x - \beta) + [\cos(k_y d_y - \gamma) - \cos(k_y d_y + \gamma)]^2}$ with $f = t_x/t_y$. The Brillouin zone is $-\pi/2d_x \leq k_x \leq \pi/2d_x$, $-\pi/d_y \leq k_y \leq \pi/d_y$. Weyl nodes occur at $(-\pi/2d_x + \beta/d_x, 0)$ and $(-\pi/2d_x + \beta/d_x, \pm\pi)$, among which there are only two inequivalent points. This model has a composite symmetry as $\Gamma' = (e^{2i\beta})^{i_x} \sigma_x K T_{\mathbf{a}_1/2}$ and $\Gamma'^2 = e^{2i\beta} T_{\mathbf{a}_1}$. In momentum space, the wave vectors are transformed as follows $\Gamma' : (k_x, k_y) \rightarrow (2\beta/d_x - k_x, -k_y)$. For the $0 < \beta \leq \pi/2$ case, the Γ' -invariant points in the Brillouin zone are $(-\pi/2 + \beta/d_x, 0)$, $(-\pi/2 + \beta/d_x, \pm\pi)$, $(\beta/d_x, 0)$, $(\beta/d_x, \pm\pi)$ and for the $\pi/2 < \beta < \pi$ case they are $(-\pi/2 + \beta/d_x, 0)$, $(-\pi/2 + \beta/d_x, \pm\pi)$, $((\beta - \pi)/d_x, 0)$, $((\beta - \pi)/d_x, \pm\pi)$. Here, only at points $(-\pi/2 + \beta/d_x, 0)$, $(-\pi/2 + \beta/d_x, \pm\pi)$, the Bloch wave functions $\Psi_{\mathbf{k}}(\mathbf{r})$ and $\Gamma'\Psi_{\mathbf{k}}(\mathbf{r})$ are orthogonal, i.e., the degeneracies at these points are protected by GCT symmetry, which is consistent with the observation of the dispersion of Model 2.

Model 3 also have two sublattices and each sublattice has the unit lattice vectors $\mathbf{a}_1'' = (d_x, -d_y)$ and $\mathbf{a}_2'' = (d_x, d_y)$. In reciprocal lattice space, the unit wave vectors are $\mathbf{b}_1'' = (\pi/d_x, -\pi/d_y)$ and $\mathbf{b}_2'' = (\pi/d_x, \pi/d_y)$. The tight-binding Hamiltonian can be written as $H'' = -\sum_{i \in A} [J_{i,i+\hat{x}} a_{i+\hat{x}}^\dagger b_{i+\hat{x}} + J_{i,i+\hat{y}} a_{i+\hat{y}}^\dagger b_{i+\hat{y}} + J_{i+\hat{x},i+\hat{x}+\hat{y}} b_{i+\hat{x}}^\dagger a_{i+\hat{x}+\hat{y}} + J_{i+\hat{x},i+2\hat{x}} b_{i+\hat{x}}^\dagger a_{i+2\hat{x}} + \text{H.c.}]$ with $J_{i,i+\hat{x}} = t_x e^{-i\gamma}$ for $i \in A$ and $t_x e^{i\gamma}$ for $i \in B$, $J_{i,i+\hat{y}} = t_y e^{i\gamma}$ for $i \in A$ and $t_y e^{-i\gamma}$ for $i \in B$, where $0 < \gamma < \pi/2$. The spectrum has the form as $E''(\mathbf{k}) = \pm 2\sqrt{\cos^2 \gamma \Omega_+^2 + \sin^2 \gamma \Omega_-^2}$ with $\Omega_+ = t_x \cos(k_x d_x) + t_y \cos(k_y d_y)$ and $\Omega_- = t_x \cos(k_x d_x) - t_y \cos(k_y d_y)$. Weyl nodes occur at $(\pm\pi/2d_x, \pm\pi/2d_y)$ in the Brillouin zone, among which there are only two inequivalent Weyl nodes. The symmetry operator is $\Gamma'' = \sigma_x K T_{(\mathbf{a}_1'' + \mathbf{a}_2'')/2}$ and its square is $\Gamma''^2 = T_{\mathbf{a}_1'' + \mathbf{a}_2''}$. In momentum space, the wave vectors are transformed as follows, $\Gamma'' : (k_x, k_y) \rightarrow (-k_x, -k_y)$. The Γ'' -invariant points in the Brillouin zone are $(\pm\pi/2d_x, \pm\pi/2d_y)$ and $(0, 0)$. But only degeneracies at $(\pm\pi/2d_x, \pm\pi/2d_y)$ are protected by GCT symmetry, which is consistent with the dispersion calculated.

Remarks and conclusion.—The models investigated above can be realized in optical lattice with laser-assisted tunneling[16]. The GCT symmetry is related with various branches of physics. For example, besides in optical lattices, Model 2 with $\beta = \gamma = \pi/2, d_x = d_y$ and Model 3 with $\gamma = \pi/4, d_x = d_y$ are just the π -flux states in spin liquid[17] and high temperature superconductors[18], respectively. Three-dimensional Weyl semimetals investigated in Reference [10] are also protected by GCT symmetry. Thus, GCT symmetry are ubiquitous in physics, in particular condensed matter physics, and has a close relation with the existence of Weyl nodes.

In summary, we have studied the three optical lattice models that support the existence of Weyl semimetals. We found that there exists a novel symmetry, GCT symmetry in these models. GCT symmetry is an antiunitary symmetry and responsible for point degeneracies of Weyl nodes. We have discussed the dispersion relations of these models and analyzed the chirality of Weyl nodes. Our study on the relation between GCT symmetry and Weyl nodes gives a clue to search for Weyl semimetals and an insight on interpreting Weyl semimetals. The study of GCT symmetry is also helpful to understanding the essence of spin liquids and high temperature superconductors.

We acknowledge support from the National Natural Science Foundation of China under Grants No. 11004028 and No. 11274061.

* Electronic address: jmhhou@seu.edu.cn

- [1] M.Z. Hasan and C.L. Kane, Rev. Mod. Phys. **82**, 3045 (2010).
- [2] X.L. Qi and S.C. Zhang, Rev. Mod. Phys. **83**, 1057 (2011).
- [3] X. Wan, A.M. Turner, A. Vishwanath, and S.Y. Savrasov, Phys. Rev. B **83**, 205101 (2011).
- [4] G. Xu, H. Weng, Z. Wang, X. Dai, and Z. Fang, Phys. Rev. Lett. **107**, 186806 (2011).
- [5] A.A. Burkov, M.D. Hook, and L. Balents, Phys. Rev. B **84**, 235126 (2011).
- [6] A.A. Burkov and L. Balents, Phys. Rev. Lett. **107**, 127205 (2011).
- [7] C. Fang, M.J. Gilbert, X. Dai, and B.A. Bernevig, Phys. Rev. Lett. **108**, 266802 (2012).
- [8] A.A. Zyuzin *et al.*, Phys. Rev. **85**, 165110 (2012).
- [9] K. Sun *et al.*, Nat. Phys. **8**, 67 (2012).
- [10] J.H. Jiang, Phys. Rev. A **85**, 033640 (2012).
- [11] P. Hosur, S.A. Parameswaran, and A. Vishwanath, Phys. Rev. Lett. **108**, 046602 (2012).
- [12] P. Delplace *et al.*, Europhys. Lett. **97**, 67004 (2012).
- [13] H.B. Nielsen and N. Ninomiya, Nucl. Phys. **B185**, 20 (1981); *ibid.* **B193**, 173 (1981).
- [14] C. Herring, Phys. Rev. **52**, 365 (1937).
- [15] L. Balents, Phys. **4**, 36 (2011).
- [16] J.M. Hou, W.X. Yang and X.J. Liu, Phys. Rev. A **79**, 043621 (2009).

- [17] X.G. Wen, *Quantum Field Theory of Many-Body Systems* (1988).
(Oxford University Press, New York, 2004).
- [18] I. Affleck and J.B. Marston, Phys. Rev. B **37**, 3774